JOURNAL OF BACTERIOLOGY, Nov. 2003, p. 6255–6261 Vol. 185, No. 21
0021-9193/03/$08.00+0 DOI: 10.1128/JB.185.21.6255–6261.2003

Morphogenesis of *Bacillus* Spore Surfaces

Venkata G. R. Chada,[1] Erik A. Sanstad,[2] Rong Wang,[1] and Adam Driks[2]*

Department of Biological, Chemical, and Physical Sciences, Illinois Institute of Technology, Chicago, Illinois 60616,[1] and Department of Microbiology and Immunology, Loyola University Medical Center, Maywood, Illinois 60153[2]

Received 2 June 2003/Accepted 13 August 2003

Spores produced by bacilli are encased in a proteinaceous multilayered coat and, in some species (including *Bacillus anthracis*), further surrounded by a glycoprotein-containing exosporium. To characterize bacillus spore surface morphology and to identify proteins that direct formation of coat surface features, we used atomic-force microscopy (AFM) to image the surfaces of wild-type and mutant spores of *Bacillus subtilis*, as well as the spore surfaces of *Bacillus cereus* 569 and the Sterne strain of *Bacillus anthracis*. This analysis revealed that the coat surfaces in these strains are populated by a series of bumps ranging between 7 and 40 nm in diameter, depending on the species. Furthermore, a series of ridges encircled the spore, most of which were oriented along the long axis of the spore. The structures of these ridges differ sufficiently between species to permit species-specific identification. We propose that ridges are formed early in spore formation, when the spore volume likely decreases, and that when the spore swells during germination the ridges unfold. AFM analysis of a set of *B. subtilis* coat protein gene mutants revealed three coat proteins with roles in coat surface morphology: CotA, CotB, and CotE. Our data indicate novel roles for CotA and CotB in ridge pattern formation. Taken together, these results are consistent with the view that the coat is not inert. Rather, the coat is a dynamic structure that accommodates changes in spore volume.

Bacterial spores are dormant cells produced by a variety of bacilli and clostridia in response to starvation. They can endure a wide range of extreme environmental stresses while retaining the capacity to return to vegetative growth (a process called germination) almost immediately once the nutrient returns to the environment (32). These remarkable characteristics allow pathogenic spores to serve as potent biological weapons (11, 50).

The spore is built as an internal double membrane-bound compartment, called the forespore, within a rod-shaped cell. Over the course of several hours, critical protective structures assemble inside of and around the forespore, with the final step being lysis of the surrounding cell and liberation of the now mature spore (36). Spore dormancy and resistance depend on the partial dehydration of the interior compartment of the spore, known as the core, that houses the spore chromosome. This occurs about mid-way in sporulation. The completed spore is encased in a multilayered protein shell known as the coat, which contributes both to spore protection and to germination (1, 9, 12, 19). In some species, including *Bacillus subtilis*, the coat is the outermost layer of the spore. In others, including *Bacillus anthracis* and *Bacillus cereus*, there exists an additional layer, called the exosporium, which encases the spore (3, 16, 20, 34). The exosporium is a pleiomorphic glycoprotein shell whose protein components are beginning to be identified (5, 45, 46, 49a) and which is separated from the coat by a significant gap. The role of the exosporium is unknown. When germination is triggered, water enters the spore core, which swells and, ultimately, the spore converts into a vegetative cell.

At least 40, and perhaps as many as 60, protein species are present in the coat (28, 29). In several species, including *B. subtilis* and, most likely, *B. anthracis* and *B. cereus*, these proteins are organized into two major layers, called the inner and outer coats, which can be seen by thin-section electron microscopy (1, 11, 52). In *B. subtilis*, the coat protein CotE sits at the interface between the inner and outer coat layers (13) and directs assembly (but not, apparently, the synthesis) of a large subset of coat proteins, including most or all of the outer coat proteins (2, 30, 55). CotE is one of a small group of proteins known to direct coat protein deposition. Most of the remaining coat proteins have less important or no detectable roles in coat assembly (12, 19, 48). Although the current model of coat assembly provides a reasonable understanding of the formation of the coat layers (12, 19, 48), it does not address how assembly within a layer is controlled. Importantly, it is unknown how proteins making up the very outermost layer of the coat (i.e., spore surface proteins) come to be organized.

Atomic-force microscopy (AFM) has been widely used in structural studies of biological systems (14, 15, 18, 37, 44). In the present study, we use AFM to characterize spore surface features and to discover proteins that control their assembly. These findings identify novel roles for known coat proteins in directing coat surface architecture and suggest that the coat is a flexible structure designed to accommodate the changes in spore volume that occur during spore maturation and germination.

MATERIALS AND METHODS

All *B. subtilis* strains are congenic with PY79 (54). We used the Sterne strain of *B. anthracis* and *B. cereus* strain 569. To generate a *cotQ*-null mutation in *B. subtilis*, we used PCR to amplify nucleotides 45 to 561 of the *cotQ* (*yvdP*) open reading frame (29) from chromosomal DNA with AAAAAAGGATCCCCCCG GCTATACAGAGGC (the *Bam*HI site is underlined) and AAAAAAGTCGA CGTTACCTCCTCCTCCGCC (the *Sal*I site is underlined) as primers. We digested the product with *Bam*HI and *Sal*I, and ligated it to similarly digested pAGS04 (30). We used the resulting plasmid to transform strain PY79, selecting

* Corresponding author. Mailing address: Department of Microbiology and Immunology, Loyola University Medical Center, 2160 S. First Ave., Maywood, IL 60153. Phone: (708) 216-3706. Fax: (708) 216-9574. E-mail: adriks@lumc.edu.

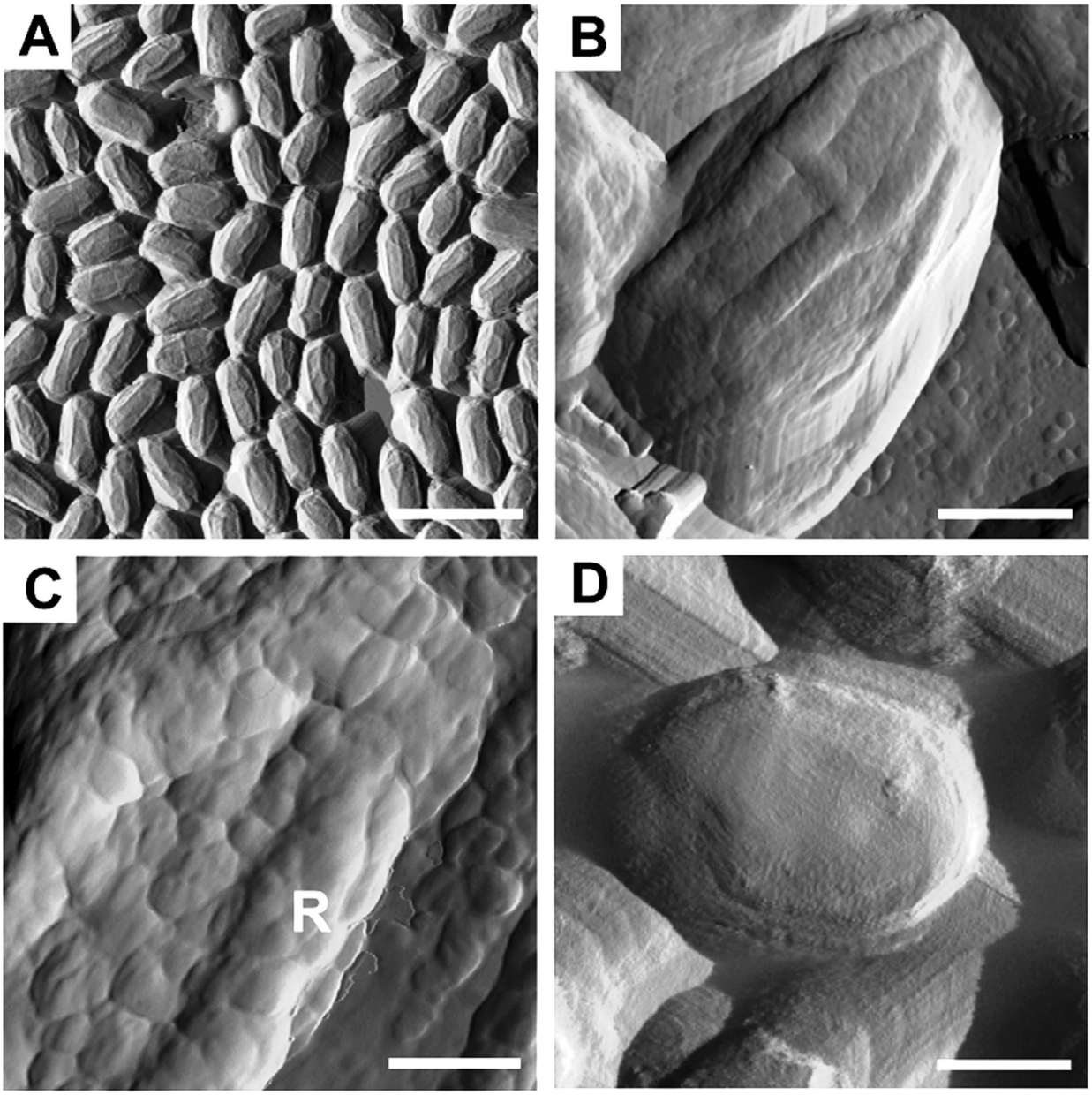

FIG. 1. AFM analysis of *B. subtilis* spores. Spores were imaged by contact (A) or tapping (B to D) mode, and amplitude image information was collected. The spore in panel D was germinated by exposure to LB medium. Bars: 2.25 μm (A), 375 nm (B), 125 nm (C), 583 nm (D). The "R" in panel C indicates a ridge.

for a single crossover (Campbell-type) integration, thereby disrupting *cotQ*. We confirmed by PCR that integration occurred as expected and showed that CotQ was no longer present in the extractable spore fraction by sodium dodecyl sulfate-polyacrylamide gel electrophoresis (data not shown). Sporulation, germination, and Western blot analysis were performed as described previously (4). AFM measurements were carried out by using a Digital Instruments (Santa Barbara, Calif.) Nanoscope IIIa with a J-scanner (maximum scan range of 150 × 150 μm^2). Fifty microliters of an aqueous spore suspension was spread on a 1-cm-by-1-cm silicon wafer, which was then mounted onto a standard sample holder. After we allowed the spores to settle on the substrate, the sample was placed in the AFM chamber for imaging. Commercial single crystal silicon cantilevers were used to acquire images in air tapping mode, which was performed at a resonant frequency of ~250 kHz. Images were obtained with 512 × 512 points at a scanning rate of 1 Hz. Dormant spores were imaged under ambient conditions after drying in air. Germinated spores were imaged in Luria-Bertani (LB) medium by using oxide sharpened Si_3N_4 tips, operating at a thermal resonance frequency of 8 to 10 kHz. The image in Fig. 1A was obtained in air contact mode, with a silicon nitride tip.

RESULTS

***B. subtilis* spore surface morphology.** We characterized the *B. subtilis* spore surface by tapping-mode AFM of air-dried samples (6). For this and every other AFM experiment, we examined a minimum of 1,000 spores. We used tapping mode instead of contact mode because the transient contact of the tip with the surface in tapping mode is likely to reduce tip-induced artifacts (44). When we used contact mode, the large-

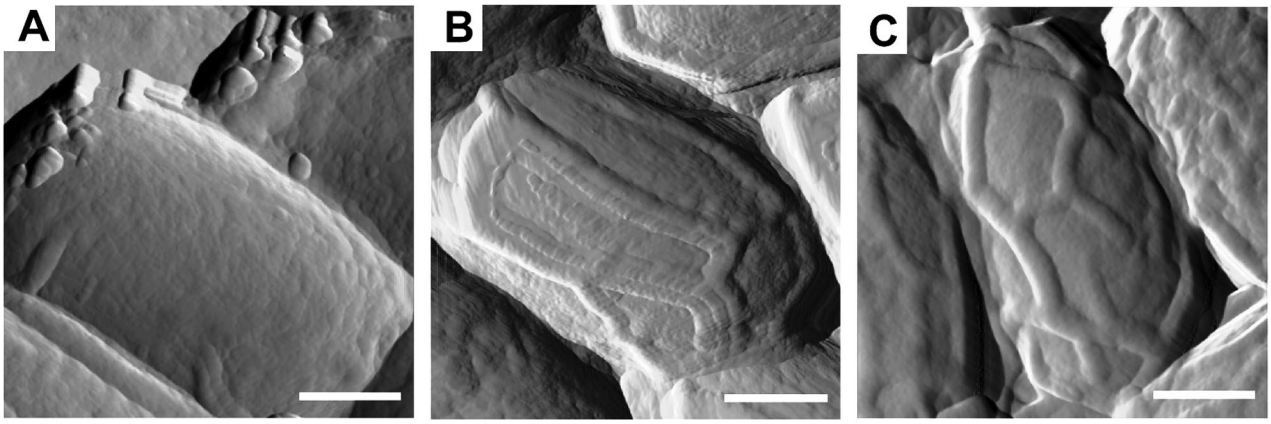

FIG. 2. AFM analysis of *B. anthracis* and *B. cereus* spores. Amplitude images of *B. anthracis* (A and B) or *B. cereus* (C) spores were collected in tapping mode. Spores with (A) or without (B and C) an exosporium are shown. Bars: 375 nm (A and C), 382 nm (B).

scale images were similar to those captured in the tapping mode (compare Fig. 1A and B). However, at a small scale, contact-mode images showed scan lines across the spore surface due to tip scratching (data not shown), which may indicate that the spore surface is relatively soft. The major artifact we encountered appeared when we imaged spore edges, where the tip is subject to abrupt changes in Z-position during scanning (51) due to very large differences in height between sample and substrate. However, this artifact is negligible when the tip scans the spore surface, where the height differences are <100 nm. Therefore, this artifact does not affect our conclusions. We captured height and amplitude images simultaneously. We measured relative heights of features by using the height images (not shown) but present the amplitude images, which are derived from the height images and highlight the surface features. Typically, we found spores to be, on average, ca. 1.2 μm long and 0.8 μm wide. The most prominent features were a series of ridges of about 85 ± 5 nm in thickness and about 12 ± 4 nm in height (Fig. 1B). The majority of ridges on any given spore typically extended along the long axis. Similar ridges have been seen by scanning electron microscopy, as well as by freeze-etch methods, in a variety of species, including *B. subtilis* (1, 7, 21). We note that our data, in contrast to those studies, were collected from entirely unfixed spores.

We found that the *B. subtilis* spore surface was studded by a series of small circular bumps, most of which are 7 to 20 nm in diameter (Fig. 1B and C). A smaller number of larger bumps, varying in diameter from 20 to 40 nm, were also present, largely on the ridges. Therefore, on average, a spore is covered by ca. 5,500 bumps. It is extremely likely that pores are present on the coat surface, since germinant molecules must penetrate the coat to reach internally located receptors (22, 35). Possibly, pores reside in spaces between the bumps. If this is true, then the outer diameter of the pores are probably 24 nm or smaller. One of the functions of the coat is to exclude large toxic enzymes, such as lysozyme (1). We note that, since the radius of gyration of lysozyme is ca. 2 nm (43), it is likely that pore diameters constrict at more interior positions.

***B. anthracis* spore surface morphology.** To explore the generality of our findings, we examined the *B. anthracis* (Sterne) coat surface. *B. anthracis* spores possess an exosporium that should obscure the coat. Consistent with this, we found that the spores fell into two morphological classes. The first (ca. 77%) were, on average, 1.27 μm long and 0.74 μm wide and did not possess ridges or bumps like those on the *B. subtilis* surface (Fig. 2A). Instead, the bumps appeared flatter and were between 8 and 40 nm in diameter. We interpret this to mean that these spores possessed an exosporium. Spores in the second morphological class were somewhat larger (1.47 μm long and 0.76 μm wide, on average) and, like *B. subtilis*, possessed ridges and bumps (Fig. 2B). We do not understand the cause of the somewhat larger size of these spores. The bumps were mostly between 15 and 25 nm in diameter but, as with *B. subtilis*, a small population of larger bumps, ranging from 20 to 40 nm in diameter, was present on the ridges. Also like *B. subtilis*, the *B. anthracis* spore ridges largely spanned the long axis. We infer that these spores had lost their exosporia during culturing or preparation for AFM analysis. Strikingly, and in contrast to *B. subtilis*, in ca. 85% of the *B. anthracis* spores without exosporia, we found structures that resembled two ridges in close apposition (Fig. 2B). Taken as a whole, these data indicate that, although *B. anthracis* spore surfaces grossly resemble those of *B. subtilis*, AFM analysis identifies features that distinguish these species.

***B. cereus* spore surface morphology.** To learn whether the surface morphology of *B. anthracis* spores can be used to distinguish closely related species, we also characterized the surface of spores of *B. cereus*, a very close relative of *B. anthracis* (17, 25, 38, 39). As with *B. anthracis*, we found that *B. cereus* spores fell into two classes. About half appeared to possess exosporia, since they had relatively smooth surfaces with very densely and uniformly packed spherical bumps (10 to 25 nm in diameter) and did not possess ridges (data not shown). These spores were 1.20 μm long and 0.75 μm wide, on average. The second group of spores (Fig. 2C) were larger (1.60 μm long and 0.90 μm wide, on average) and had ridges. As for the case of *B. anthracis*, we do not know why spores in this class were larger. The diameters of the bumps were uniform (7 to 13 nm) over the entire spore surface. The ridges were morphologically distinct from those of *B. anthracis* or *B. subtilis*. First, the ridges did not resemble two closely positioned ridges. Second, the

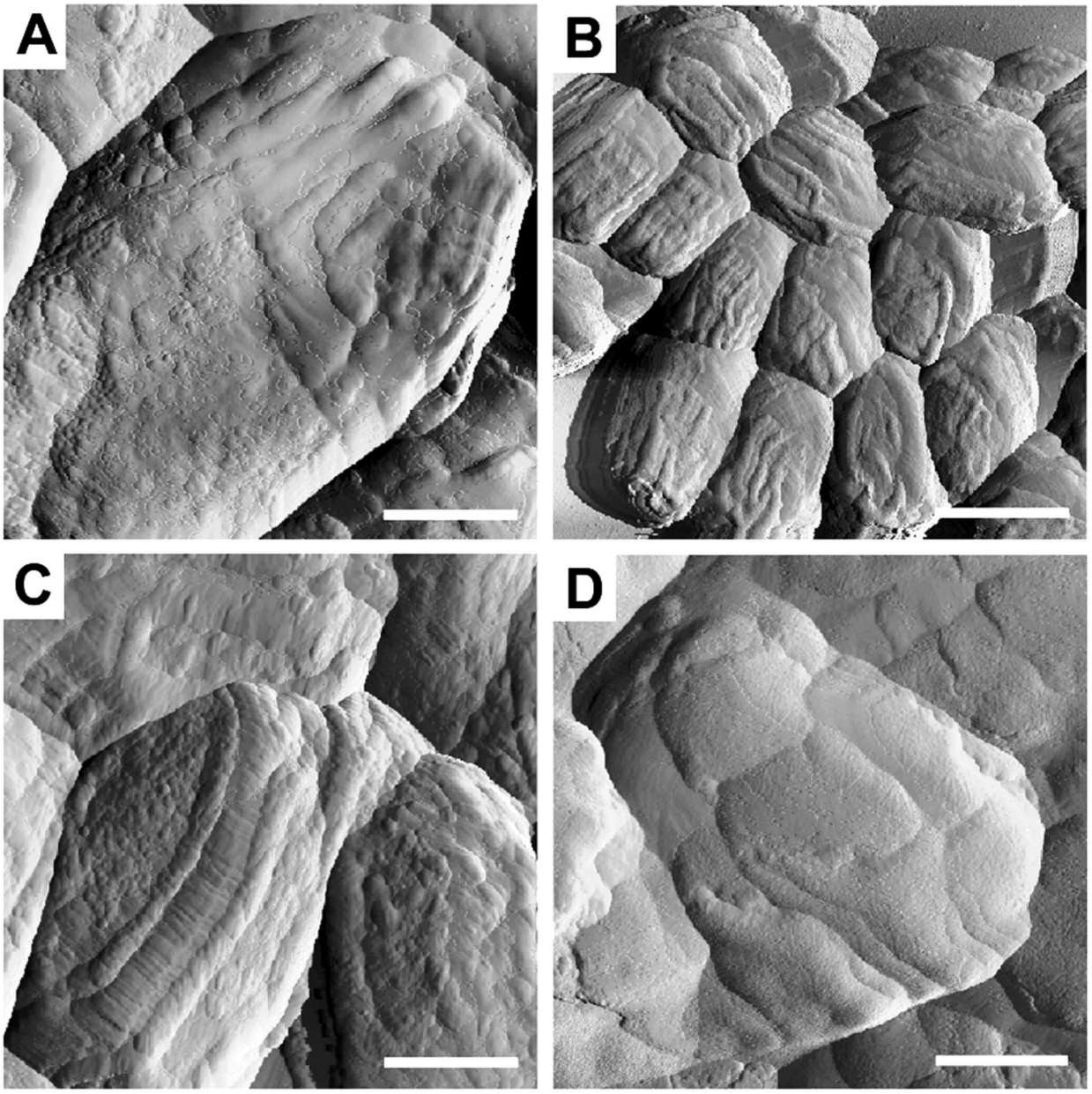

FIG. 3. AFM analysis of *B. subtilis* mutant spores. Amplitude images of *cotE* (A), *cotA* (B), *cotB* (C) or *cotA cotB* (D) spores were collected in tapping mode. Bars: 350 nm (A), 2.25 μm (B), 410 nm (C), 468 nm (D).

ridges did not transit along the long axis of the spore in straight lines but, instead, possessed angular bends.

Roles of coat proteins in *B. subtilis* coat surface morphology. To identify coat proteins with roles in spore surface morphology, we used AFM to image the surfaces of *B. subtilis* spores bearing null mutations in each of several coat protein genes. We first analyzed *cotE* spores. In *cotE* spores, the ridges and the relatively regular pattern of bumps were greatly reduced or entirely absent (Fig. 3A). Instead, the spore surface was populated by both small bumps and somewhat broader, irregularly shaped elevated areas. Given the role of CotE in outer coat assembly (55), we infer that this surface is that of the inner coat.

To learn how CotE influences spore surface morphology, we analyzed the surfaces of spores missing one or another protein whose assembly is CotE dependent (2, 30, 55). All of the strains analyzed are congenic with the wild-type background PY79 (54). We found that most of the mutants in this set, including those that do not produce the coat proteins CotG, CotH, CotR, CotQ, CotS, and YaaH (27, 29, 30, 33, 41, 47), had no obvious effect on coat surface morphology (data not shown). In contrast, we discovered that the absence of the CotE-controlled proteins CotA and CotB significantly affected the ridges. CotA is a multi-copper oxidase (23, 31). Strikingly, in *cotA* spores, the ridges tended to branch more than in the wild type and varied in thickness, ranging from 35 to 60 nm

(Fig. 3B). In *cotB* spores, the ridges frequently appeared as parallel pairs, connected by a series of fine ridges (Fig. 3C). This morphological role for CotB is noteworthy in light of evidence that CotB is on the spore surface (24). No enzymatic role for CotB is known. It is noteworthy that mutations in *cotG* or *cotH* do not have more severe effects, given that in spores from these strains, the presence of CotB in the extractable fraction of the spore coat is diminished or eliminated (33, 41). We speculate that although the quantity of extractable CotB in these strains is reduced, enough is assembled to permit ridge formation. In *cotA cotB* spores (which sporulate normally [data not shown]), we did not observe ridges or bumps (Fig. 3D). Rather, the spore surface was largely smooth but was tessellated by a small number of relatively large, roughly square patches. Previous studies showed that *cotA* or *cotB* mutant spores are indistinguishable from the wild type in their germination properties (8). We found that *cotB* and *cotA cotB* spores were also indistinguishable from the wild type when analyzed by thin-section electron microscopy (data not shown), and we infer that *cotA* spores are indistinguishable as well. Therefore, the effect of the double mutant on surface morphology is not a consequence of a gross change in the morphology of the underlying coat layers.

What is the function of the ridges? To address this question, we first considered electron microscopic observations spanning decades, indicating that folds in the coat layers (presumably equivalent to the ridges we detected by AFM) appear late in sporulation, are maintained during dormancy and, finally, disappear upon germination (9, 42). Next, we noted that, most likely, the core volume contracts during dehydration and then increases during germination (42). We speculated, therefore, that an important function of the ridges might be to ensure that the coat is sufficiently flexible to accommodate these volume changes. If so, we reasoned that the pattern of ridges should reflect the nature of the contractile force vectors produced during core dehydration.

To learn whether this notion is plausible, we constructed a simple dynamic model for ridge formation that assumes that the coat is a largely homogenous material, that the inward contractile forces are uniform, and that the system tends toward the lowest Gibbs free energy. First, we consider an idealized spore to be an ellipsoid formed from the rotation of an ellipse along its long axis. The surface area of the ellipsoid is $A = 2\pi(b^2 + ab)$, with "a" and "b" representing the long and short axis, respectively. The full differentiation of the surface area is $dA = 2\pi[(2b + a)db + b\,da]$, implying $(\partial A/\partial b)_a = 2\pi(2b + a)$, and $(\partial A/\partial a)_b = 2\pi b$. Since $a > 0$ and $b > 0$, it follows that $(\partial A/\partial b)_a > (\partial A/\partial a)_b$. That is, the change of surface area resulting from a change in b is larger than that caused by changes in a. The work produced by surface tension, resulting from an infinitesimal change of the ellipsoid surface area, is $dW = \gamma dA$, where γ is the surface tension, an intrinsic property of the ellipsoid material. Thus, the change of free energy of the system is: $dG = -SdT + VdP + \sum_i \mu_i\, dn_i + \gamma dA$. Assuming this takes place under ambient conditions (at room temperature and 1 atm pressure) and that no matter exchange between the system and surrounding environment occurs, i.e., $dn_i = 0$, then $dG = \gamma dA$. If the Gibbs free energy decreases, i.e., $dG < 0$, the change will be spontaneous and, therefore, energetically favored. Thus, the maximum decrease of surface area will be energetically preferred by the system. Given that $(\partial A/\partial b)_a > (\partial A/\partial a)_b$, this model predicts that during dehydration, ridges will form preferentially along the long axis, a finding consistent with our observations.

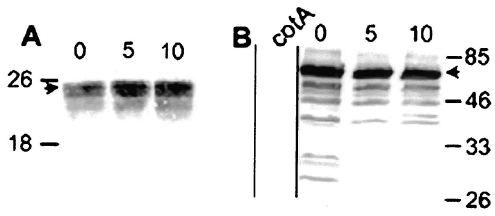

FIG. 4. Western blot analysis of coat protein cleavage during germination. Proteins were extracted from wild-type spores before (lanes 0) or various times after (indicated in minutes above the lanes) resuspension in LB medium (to initiate germination) or from a *cotA* mutant (8) (left-most lane in panel B), fractionated by sodium dodecyl sulfate–15% polyacrylamide gel electrophoresis, and subjected to Western blot analysis with anti-CotE (A) or anti-CotA antibodies (B). Arrowheads indicate full-length versions of each protein. Molecular masses are indicated in kilodaltons on either side of the gels.

To test whether ridges are lost after rehydration, we imaged germinated *B. subtilis* spores. We observed that within 10 min of exposure to rich medium, the spores increased in size to about 1.8 μm long and 1.2 μm wide on average and the ridges disappeared (Fig. 1D). This finding is consistent with our expectation (and previous observations [42]) that the ridges disappear as the spore swells.

Cleavage of coat proteins during germination. Identification of coat proteins with roles in spore surface morphology raised the possibility that some of these proteins are also involved in ultrastructural changes associated with germination. To test this, we used Western blot analysis of spore extracts to learn whether the molecular masses of CotE or CotA change during germination in *B. subtilis*. Negative control experiments showed that these sera do not react with proteins extracted from *cotE* or *cotA* strains (Fig. 4B and data not shown). Dormant spores possessed the expected full-length versions of each protein, as well as lower-molecular-mass species. After initiation of germination, we did not detect any changes in the size of CotE, even after 90 min (Fig. 4A and data not shown). In contrast, within 5 min, CotA species of between 64 and 26 kDa had altered migration or were no longer detectable (Fig. 4B).

DISCUSSION

There are three main results from the present study. First, we have identified differences in the surfaces of the coats of individual strains of three important species, indicating that AFM could be a useful tool for spore species identification in circumstances in which traditional techniques are inappropriate, such as characterization of biological weapons. Establishing this as a robust method, however, will require examination of a larger number of isolates of each species. Second, we have identified roles for the coat proteins CotA, CotB, and CotE in spore surface morphology in *B. subtilis*. Thus, at least some of the protein determinants of spore surface architecture likely differ from those that direct the layered structure of the coat (such as CotH [56]) studied previously by thin-section electron

microscopy, and visa versa. Third, the electrophoretic pattern of CotA species in the coat changes soon after germination is triggered. Possibly, proteolysis of CotA is required for either unfolding or shedding of the coat.

We do not know the molecular basis for the effects of CotA or CotB, but their roles are likely to be complex, given that null alleles of each gene alter the ridge pattern rather than simply reduce or eliminate the ridges. CotA and CotB are not the only CotE-dependent factors guiding surface morphogenesis, since the *cotA cotB* phenotype differs from that of a *cotE* spore. The likelihood that no single protein directs ridge formation indicates that ridges are an emergent phenomenon (49). Other morphological and functional aspects of the coat might be emergent as well. In this regard, it is noteworthy that mutations in any one of a large number of coat protein genes have no detectable consequence by AFM (the present study) or by traditional assays of structure and function (12, 19, 48). We further note that we have not tested all plausible surface morphogenetic factors. Additional genes with possible roles include *cotM*, *cotX*, *cotY*, and *cotZ* and the *cge* genes, whose products may glycosylate the spore surface (40).

We speculate that ridge formation is a direct consequence of core contraction during dehydration. This could occur in at least two ways. First, the coat could act as an elastic material and, therefore, form folds during dehydration because core contraction allows it to reach a lower energy state. An alternative view is that connections between the inner surface of the coat and the outer surface of the cortex (or the outer forespore membrane, should it exist at this point in sporulation [9]) allow the force of core contraction to actively pull the coat inward. Both scenarios are consistent with our mathematical model.

These considerations give rise to a novel view of the coat. From this perspective, the coat is initially assembled as a ridgeless shell that follows the smooth contours of the immature forespore protoplast. Because of the relatively large surface area of the forespore prior to dehydration, the coat is in an extended state. The ridges form only after the core volume decreases during dehydration. If the coat behaves as an elastic material, then coat protein monomers must be synthesized in a relatively high-energy state and the spring-like nature of the coat appears only after assembly is largely or entirely complete. The notion that, prior to dehydration, the coat is in a metastable state brings to mind the assembly of the tail sheath of bacteriophage T4 (26). The view that the coat is flexible, along with a recent study by Westphal et al. (53; see also reference 10), may help account for a type of variability commonly seen in thin-section electron micrographs of spores; typical fields show spores in which the ridge number and shape varies significantly. These authors found that spore size changes dynamically as a function of relative humidity. Small differences in dehydration and/or coat formation from spore to spore could account for much of this variability. Indeed, it would seem plausible that coat flexibility provides a mechanism to accommodate changes in environmental humidity.

Since our mathematical model indicates that the ridges form as expected if the coat is a homogeneous material, then one interpretation of the *cotA* and *cotB* phenotypes is that the corresponding proteins are required for coat homogeneity. Importantly, neither protein is essential for ridge formation per se, since ridges are still formed, albeit aberrantly, when these proteins are missing. This is in contrast to CotE, which we infer has additional roles. Consistent with the possibility that CotE helps retain an elastic property of the coat, thin-section electron microscopy shows that, in *cotE* mutant spores, the coat is no longer in close apposition to the cortex surface (2, 9). A homologue of CotE, as well as a protein resembling CotB, is present in both *B. anthracis* and *B. cereus* (29). Characterization of the surfaces of the relevant mutants of these species is ongoing in our laboratories, and we expect these studies to help clarify the commonalities and differences in the spore coat assembly programs of these organisms.

Previous analysis by freeze-etch electron microscopy suggests that the coat layers are sheets of proteins arranged in a crystalline or partially crystalline lattice (1, 21). We were unable to detect these features. These differences could be the consequence of the unhydrated state of most of our samples or that the surface layer we imaged had been removed during processing in previous experiments. Although we feel that AFM provides a uniquely reliable image of the coat surface due to the minimal specimen preparation involved, we also believe that freeze-etch methodology will be critical for further characterization of spore surfaces and may reveal features undetected in the present study.

ACKNOWLEDGMENTS

We thank Michele Otte for constructing the *cotQ* mutant. We are grateful to Jean Greenberg, David Keating, Zhifeng Shao, and Karen Visick for helpful comments on the manuscript.

This work was supported by grants NER0103080 from the NSF (R.W.) and GM53989 from the NIH (A.D.).

REFERENCES

1. **Aronson, A. I., and P. Fitz-James.** 1976. Structure and morphogenesis of the bacterial spore coat. Bacteriol. Rev. **40:**360–402.
2. **Bauer, T., S. Little, A. G. Stöver, and A. Driks.** 1999. Functional regions of the *Bacillus subtilis* spore coat morphogenetic protein CotE. J. Bacteriol. **181:**7043–7051.
3. **Beaman, T. C., H. S. Pankratz, and P. Gerhardt.** 1972. Ultrastructure of the exosporium and underlying inclusions in spores of *Bacillus megaterium* strains. J. Bacteriol. **109:**1198–1209.
4. **Catalano, F. A., J. Meador-Parton, D. L. Popham, and A. Driks.** 2001. Amino acids in the *Bacillus subtilis* morphogenetic protein SpoIVA with roles in spore coat and cortex formation. J. Bacteriol. **183:**1645–1654.
5. **Charlton, S., A. J. Moir, L. Baillie, and A. Moir.** 1999. Characterization of the exosporium of *Bacillus cereus*. J. Appl. Microbiol. **87:**241–245.
6. **Colton, R. J., A. Engel, J. E. Frommer, H. E. Gaub, A. A. Gewirth, R. Guckenberger, W. J. Rabe, M. Heckl, and B. Parkinson.** 1998. Procedures in scanning probe microscopy. John Wiley & Sons, Ltd., Chichester, England.
7. **Comas-Riu, J., and J. Vives-Rego.** 2002. Cytometric monitoring of growth, sporogenesis and spore cell sorting in *Paenibacillus polymyxa* (formerly *Bacillus polymyxa*). J. Appl. Microbiol. **92:**475–481.
8. **Donovan, W., L. Zheng, K. Sandman, and R. Losick.** 1987. Genes encoding spore coat polypeptides from *Bacillus subtilis*. J. Mol. Biol. **196:**1–10.
9. **Driks, A.** 1999. The *Bacillus subtilis* spore coat. Microbiol. Mol. Biol. Rev. **63:**1–20.
10. **Driks, A.** 2003. The dynamic spore. Proc. Natl. Acad. Sci. USA **100:**3007–3009.
11. **Driks, A.** 2002. Maximum shields: the armor plating of the bacterial spore. Trends Microbiol. **10:**251–254.
12. **Driks, A.** 2002. Proteins of the spore core and coat, p. 527–536. *In* A. L. Sonenshein, J. A. Hoch, and R. Losick (ed.), *Bacillus subtilis* and its closest relatives. American Society for Microbiology, Washington, D.C.
13. **Driks, A., S. Roels, B. Beall, C. P. J. Moran, and R. Losick.** 1994. Subcellular localization of proteins involved in the assembly of the spore coat of *Bacillus subtilis*. Genes Dev. **8:**234–244.
14. **Dufrêne, Y. F., C. J. P. Boonaert, P. A. Gerin, M. Asther, and P. G. Rouxhet.** 1999. Direct probing of the surface ultrastructure and molecular interactions of dormant and germinating spores of phanerochaete chrysosporium. J. Bacteriol. **181:**5350–5354.
15. **Fotiadis, D., S. Scheuring, S. A. Müller, A. Engel, and D. J. Müller.** 2002. Imaging and manipulation of biological structures with the AFM. Micron **33:**385–397.

16. **Gerhardt, P., and E. Bibi.** 1964. Ultrastructure of the exosporium enveloping spores of *Bacillus cereus*. J. Bacteriol. **88:**1774–1789.
17. **Helgason, E., O. A. Okstad, D. A. Caugant, H. A. Johansen, A. Fouet, M. Mock, I. Hegna, and Kolsto.** 2000. *Bacillus anthracis*, *Bacillus cereus*, and *Bacillus thuringiensis*—one species on the basis of genetic evidence. Appl. Environ. Microbiol. **66:**2627–2630.
18. **Henderson, E., P. G. Haydon, and D. S. Sakaguchi.** 1992. Actin filament dynamics in living glial cells imaged by atomic force microscopy. Science **257:**1944–1946.
19. **Henriques, A. O., and C. P. Moran, Jr.** 2000. Structure and assembly of the bacterial endospore coat. Methods **20:**95–110.
20. **Holt, S. C., J. J. Gauther, and D. J. Tipper.** 1975. Ultrastructural studies of sporulation in *Bacillus sphaericus*. J. Bacteriol. **122:**1322–1338.
21. **Holt, S. C., and E. R. Leadbetter.** 1969. Comparative ultrastructure of selected aerobic spore-forming bacteria: a freeze-etching study. Bacteriol. Rev. **33:**346–378.
22. **Hudson, K. D., B. M. Corfe, E. H. Kemp, I. M. Feavers, P. J. Coote, and A. Moir.** 2001. Localization of GerAA and GerAC germination proteins in the *Bacillus subtilis* spore. J. Bacteriol. **183:**4317–4322.
23. **Hullo, M. F., I. Moszer, A. Danchin, and I. Martin-Verstraete.** 2001. CotA of *Bacillus subtilis* is a copper-dependent laccase. J. Bacteriol. **183:**5426–5430.
24. **Isticato, R., G. Cangiano, H. T. Tran, A. Ciabattini, D. Medaglini, M. R. Oggioni, M. De Felice, G. Pozzi, and E. Ricca.** 2001. Surface display of recombinant proteins on *Bacillus subtilis* spores. J. Bacteriol. **183:**6294–6301.
25. **Ivanova, N., A. Sorokin, I. Anderson, N. Galleron, B. Candelon, V. Kapatral, A. Bhattacharyya, G. Reznik, N. Mikhailova, A. Lapidus, L. Chu, M. Mazur, E. Goltsman, N. Larsen, M. D'Souza, T. Walunas, Y. Grechkin, G. Pusch, R. Haselkorn, M. Fonstein, S. Dusko-Ehrlich, R. Overbeek, and N. Kyrpides.** 2003. Genome sequence of *Bacillus cereus* and comparative analysis with *Bacillus anthracis*. Nature **423:**87–91.
26. **King, J.** 1980. Regulation of structural protein interactions as revealed in phage morphogenesis, p. 101–132. *In* R. F. Goldberger (ed.), Biological regulation and development, vol. 2. Plenum Press, Inc., New York, N.Y.
27. **Kodama, T., H. Takamatsu, K. Asai, K. Kobayashi, N. Ogasawara, and K. Watabe.** 1999. The *Bacillus subtilis yaaH* gene is transcribed by SigE RNA polymerase during sporulation, and its product is involved in germination of spores. J. Bacteriol. **181:**4584–4591.
28. **Kuwana, R., Y. Kasahara, M. Fujibayashi, H. Takamatsu, N. Ogasawara, and K. Watabe.** 2002. Proteomics characterization of novel spore proteins of *Bacillus subtilis*. Microbiology **148:**3971–3982.
29. **Lai, E.-M., N. D. Phadke, M. T. Kachman, R. Giorno, S. Vazquez, J. A. Vazquez, J. R. Maddock, and A. Driks.** 2003. Proteomic analysis of the spore coats of *Bacillus subtilis* and *Bacillus anthracis*. J. Bacteriol. **185:**1443–1454.
30. **Little, S., and A. Driks.** 2001. Functional analysis of the *Bacillus subtilis* morphogenetic spore coat protein CotE. Mol. Microbiol. **42:**1107–1120.
31. **Martins, L. O., C. M. Soares, M. M. Pereira, M. Teixeira, T. Costa, G. H. Jones, and A. O. Henriques.** 2002. Molecular and biochemical characterization of a highly stable bacterial laccase that occurs as a structural component of the *Bacillus subtilis* endospore coat. J. Biol. Chem. **277:**18849–18859.
32. **Moir, A., B. M. Corfe, and J. Behravan.** 2002. Spore germination. Cell. Mol. Life Sci. **59:**403–409.
33. **Naclerio, G., L. Baccigalupi, R. Zilhao, M. De Felice, and E. Ricca.** 1996. *Bacillus subtilis* spore coat assembly requires *cotH* gene expression. J. Bacteriol. **178:**4375–4380.
34. **Ohye, D. F., and W. G. Murrell.** 1973. Exosporium and spore coat formation in *Bacillus cereus* T. J. Bacteriol. **115:**1179–1190.
35. **Paidhungat, M., and P. Setlow.** 2001. Localization of a germinant receptor protein (GerBA) to the inner membrane of *Bacillus subtilis* spores. J. Bacteriol. **183:**3982–3990.
36. **Piggot, P., and R. Losick.** 2002. Sporulation genes and intercompartmental regulation, p. 483–517. *In* A. L. Sonenshein, J. A. Hoch, and R. Losick (ed.), *Bacillus subtilis* and its closest relatives. American Society for Microbiology, Washington, D.C.
37. **Plomp, M., M. K. Rice, E. K. Wagner, A. McPherson, and A. J. Malkin.** 2002. Rapid visualization at high resolution of pathogens by atomic force microscopy: structural studies of herpes simplex virus-1. Am. J. Pathol. **160:**1959–1966.
38. **Priest, F. G.** 1993. Systematics and ecology of *Bacillus*, p. 3–16. *In* A. L. Sonenshein, J. Hoch, and R. Losick (ed.), *Bacillus subtilis* and other gram-positive bacteria: biochemistry, physiology, and molecular genetics. American Society for Microbiology, Washington, D.C.
39. **Read, T. D., S. N. Peterson, N. Tourasse, L. W. Baillie, I. T. Paulsen, K. E. Nelson, H. Tettelin, D. E. Fouts, J. A. Eisen, S. R. Gill, E. K. Holtzapple, O. K. OA, E. Helgason, J. Rilstone, M. Wu, J. F. Kolonay, M. J. Beanan, R. J. Dodson, L. M. Brinkac, M. Gwinn, R. T. DeBoy, R. Madpu, S. C. Daugherty, A. S. Durkin, D. H. Haft, W. C. Nelson, J. D. Peterson, M. Pop, H. M. Khouri, D. Radune, J. L. Benton, Y. Mahamoud, L. Jiang, I. R. Hance, J. F. Weidman, K. J. Berry, R. D. Plaut, A. M. Wolf, K. L. Watkins, W. C. Nierman, A. Hazen, R. Cline, C. Redmond, J. E. Thwaite, O. White, S. L. Salzberg, B. Thomason, A. M. Friedlander, T. M. Koehler, P. C. Hanna, A. B. Kolsto, and C. M. Fraser.** 2003. The genome sequence of *Bacillus anthracis* Ames and comparison to closely related bacteria. Nature **423:**81–86.
40. **Roels, S., and R. Losick.** 1995. Adjacent and divergently oriented operons under the control of the sporulation regulatory protein GerE in *Bacillus subtilis*. J. Bacteriol. **177:**6263–6275.
41. **Sacco, M., E. Ricca, R. Losick, and S. Cutting.** 1995. An additional GerE-controlled gene encoding an abundant spore coat protein from *Bacillus subtilis*. J. Bacteriol. **177:**372–377.
42. **Santo, L. Y., and R. H. Doi.** 1974. Ultrastructural analysis during germination and outgrowth of *Bacillus subtilis* spores. J. Bacteriol. **120:**475–481.
43. **Segel, D. J., A. Bachmann, J. Hofrichter, K. O. Hodgson, S. Doniach, and T. Kiefhaber.** 1999. Characterization of transient intermediates in lysozyme folding with time-resolved small-angle X-ray scattering. J. Mol. Biol. **288:**489–499.
44. **Shao, Z., J. Mou, D. M. Czajkowsky, J. Yang, and J. Y. Yuan.** 1996. Biological atomic force microscopy: what is achieved and what is needed. Adv. Physics **45:**1–86.
45. **Steichen, C., P. Chen, J. F. Kearney, and C. L. Turnbough, Jr.** 2003. Identification of the immunodominant protein and other proteins of the *Bacillus* anthracis exosporium. J. Bacteriol. **185:**1903–1910.
46. **Sylvestre, P., E. Couture-Tosi, and M. Mock.** 2002. A collagen-like surface glycoprotein is a structural component of the *Bacillus anthracis* exosporium. Mol. Microbiol. **45:**169–178.
47. **Takamatsu, H., Y. Chikahiro, T. Kodama, H. Koide, S. Kozuka, K. Tochikubo, and K. Watabe.** 1998. A spore coat protein, CotS, of *Bacillus subtilis* is synthesized under the regulation of sigmaK and GerE during development and is located in the inner coat layer of spores. J. Bacteriol. **180:**2968–2974.
48. **Takamatsu, H., and K. Watabe.** 2002. Assembly and genetics of spore protective structures. Cell. Mol. Life Sci. **59:**434–444.
49. **Thomas, J. H.** 1993. Thinking about genetic redundancy. Trends Genet. **9:**395–399.
49a. **Todd, S. J., A. J. Moir, M. J. Johnson, and A. Moir.** 2003. Genes of *Bacillus cereus* and *Bacillus anthracis* encoding proteins of the exosporium. J. Bacteriol. **185:**3373–3378.
50. **Turnbull, P. C.** 2002. Introduction: anthrax history, disease, and ecology. Curr. Top. Microbiol. Immunol. **271:**1–19.
51. **Velegol, S. B., and B. E. Logan.** 2002. Contributions of bacterial surface polymers, electrostatics, and cell elasticity to the shape of AFM force curves. Langmuir **18:**5256–5262.
52. **Warth, A. D., D. F. Ohye, and W. G. Murrell.** 1963. The composition and structure of bacterial spores. J. Cell Biol. **16:**579–592.
53. **Westphal, A. J., P. B. Price, T. J. Leighton, and K. E. Wheeler.** 2003. Kinetics of size changes of individual *Bacillus thuringiensis* spores in response to changes in relative humidity. Proc. Natl. Acad. Sci. USA **100:**3461–3466.
54. **Youngman, P., J. B. Perkins, and R. Losick.** 1984. Construction of a cloning site near one end of Tn*917* into which foreign DNA may be inserted without affecting transposition in *Bacillus subtilis* or expression of the transposon-borne *erm* gene. Plasmid **12:**1–9.
55. **Zheng, L., W. P. Donovan, P. C. Fitz-James, and R. Losick.** 1988. Gene encoding a morphogenic protein required in the assembly of the outer coat of the *Bacillus subtilis* endospore. Genes Dev. **2:**1047–1054.
56. **Zilhao, R., G. Naclerio, A. O. Henriques, L. Baccigalupi, C. P. Moran, Jr., and E. Ricca.** 1999. Assembly requirements and role of CotH during spore coat formation in *Bacillus subtilis*. J. Bacteriol. **181:**2631–2633.